

# Calculating free energies using scaled-force molecular dynamics algorithm

By Eric Darve, Michael A. Wilson<sup>†</sup> AND Andrew Pohorille<sup>†</sup>

## 1. Motivation and objectives

One common objective of molecular simulations in chemistry and biology is to calculate the free energy difference between different states of the system of interest. Examples of problems that have such an objective are calculations of receptor-ligand or protein-drug interactions, associations of molecules in response to hydrophobic, and electrostatic interactions or partition of molecules between immiscible liquids. Another common objective is to describe evolution of the system towards a low energy (possibly the global minimum energy), “native” state. Perhaps the best example of such a problem is folding of proteins or short RNA molecules.

Both types of problems share the same difficulty. Often, different states of the system are separated by high energy barriers, which implies that transitions between these states are rare events. This, in turn, can greatly impede exploration of phase space. In some instances this can lead to “quasi non-ergodicity”, whereby a part of phase space is inaccessible on timescales of the simulation.

A host of strategies has been developed to improve efficiency of sampling the phase space. For example, some Monte Carlo techniques involve large steps which move the system between low-energy regions in phase space without the need for sampling the configurations corresponding to energy barriers (J-walking). Most strategies, however, rely on modifying probabilities of sampling low and high-energy regions in phase space such that transitions between states of interest are encouraged. Perhaps the simplest implementation of this strategy is to increase the temperature of the system. This approach was successfully used to identify denaturation pathways in several proteins, but it is clearly not applicable to protein folding. It is also not a successful method for determining free energy differences. Finally, the approach is likely to fail for systems with co-existing phases, such as water-membrane systems, because it may lead to spontaneous mixing. A similar difficulty may be encountered in any method relying on global modifications of phase space.

A new, promising technique is the multicanonical Monte Carlo method. In this algorithm, sampling of energy proportional to the Boltzmann factor is substituted by sampling from the uniform energy probability distribution. This means that multicanonical simulation corresponds to a random walk in one-dimensional energy space and, therefore, the system does not experience energy barriers. Since multicanonical weights are not known initially, they have to be estimated in the first step of the simulations. The multicanonical Monte Carlo method appears to be particularly suitable to study helix-coil transition in proteins because a single simulation can provide information about both the low-temperature, helical state and the high-temperature, disordered state.

Many problems of chemical or biological interest can be formulated in terms of evo-

<sup>†</sup> NASA Ames & UCSF

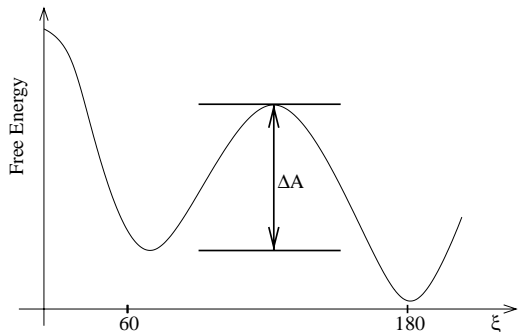
lution of a system along a small number of slow degrees of freedom in the potential of mean force exerted by the remaining coordinates. Then an effective strategy is to add to the Hamiltonian a biasing potential chosen such that free energy barriers in this reduced representation decrease. Sometimes identifying the slow degrees of freedom is not easy, especially if a formally defined reaction coordinate is sought. In many instances, however, our intuitive understanding of the problem can guide us successfully in this process. For example, transport of ions and small molecules across membranes can be well described by calculating the potential of mean force associated with moving the center of mass of the solute in the direction perpendicular to the membrane. In another example, folding of peptides or small, single-domain proteins can be studied by selecting  $\phi$ ,  $\psi$  (angles in the peptide backbone) and, possibly, some  $\chi$  angles (angle of rotation of side chains) as slow degrees of freedom.

The method of biasing potentials has several important advantages. First, using a reduced representation is very helpful in planning the simulations and analyzing their results. In fact, it can be argued that, precisely for this reason, it is extremely useful to identify the slow degrees of freedom from the very beginning. Second, if motion along only a few, selected slow degrees of freedom is modified, the chances for the correct identification of pathways along which the system evolves improve markedly. The approach also has a serious disadvantage. To design a useful biasing potential, a good, initial guess about the shape of the potential of mean force is required. If, however, no such guess is available, the approach may turn into a very frustrating experience. Unfortunately, correct estimation of the potential of mean force is often quite difficult because it depends on several contributions of different origin, such as solute-solvent interactions, solvent reorganization, and interactions between solute atoms separated by many bonds but close in space.

In this paper, we present a new approach to the problem of efficient sampling of phase space, based on the molecular dynamics (MD) algorithm in the canonical ensemble. As in the methods of biasing potential, it requires the initial identification of slow degrees of freedom. It does not, however, suffer from the main disadvantage of these methods; no prior assumptions about the shape of the potential of mean force are needed. Even without this assumption, the free energy differences between states in the reduced phase space can be calculated efficiently, perhaps even optimally.

We prove that the derivative of the free energy along a selected generalized degree of freedom can be expressed by an average force, which is a function of this coordinate, and its derivatives with respect to time and positions of the particles. Thus, it can be easily calculated numerically. If this force is scaled by  $0 \leq \alpha \leq 1$  or completely eliminated and substituted by another, suitably chosen force, sampling of the generalized coordinate improves markedly. To underscore this feature we call our approach the Scaled Force Algorithm (SFA). Even though the new force acting on the selected coordinate is not, in general, derived from a Hamiltonian, it is still possible, under appropriate conditions, to calculate the free energy change along the selected coordinate in the unmodified system.

In the next section, we present the main idea and the implementation of the method. As the test case, we selected conformational transition of 1,2-dichloroethane in water. The main body of the paper closes with the summary and the outline of future work.

FIGURE 1. Free energy  $A(\xi)$  for DCE - schematic

## 2. Thermodynamics force

We consider a system of  $N$  particles. This system can be characterized by the position of the particles  $\mathbf{x}_1, \dots, \mathbf{x}_N$  and their momenta  $\mathbf{p}_{\mathbf{x}_1}, \dots, \mathbf{p}_{\mathbf{x}_N}$ .

Very often we may be only interested in a much more limited number of degrees of freedom. Typically these degrees of freedom can be torsion angles, distances between centers of mass of molecules, distance between center of mass of a molecule and a membrane, etc. From a more abstract point of view, these can simply be viewed as functions of the position and momenta of the particles.

For simplicity we consider the case of 1,2-dichloroethane (DCE) for which we are interested in only one degree of freedom, the torsion angle  $\xi$  for the Cl-C-C-Cl bonds. It is well-known that for this case there are three stable configurations: gauche (60 deg), trans (180 deg), gauche-prime (300 deg).

The relative stability of these configurations can be obtained from the free energy  $A(\xi)$ . It can be defined as:

$$A(\xi) \stackrel{def}{=} -\kappa T \log P(\xi) + A_0 \quad (2.1)$$

where  $P(\xi)$  is the probability density function of the torsion angle  $\xi$ .  $A_0$  is an arbitrary constant. See Fig. 1 for an illustration. When the theory of transition state approximation is valid, the probability to go from one configuration, say gauche, to another configuration, say trans, is equal to:

$$P(\text{gauche} \rightarrow \text{trans}) = \frac{1}{\mathcal{N}} \exp(-\beta \Delta A)$$

where  $\Delta A$  is the energy barrier separating 60 deg from 180 deg (see Fig. 1).  $\mathcal{N}$  is a normalization factor and  $\beta \stackrel{def}{=} 1/(\kappa T)$ .

One of the usual methods to compute the free energy uses Eq. (2.1) and explicitly computes  $P(\xi)$ . Another approach consists in considering the derivative of the free energy  $dA/d\xi$ . This quantity has dimension of a force and can be viewed as the average force acting on  $\xi$ .

More precisely, the following equations can be derived. The probability density for a system at temperature  $T$  to be in state  $\mathbf{x}_1, \dots, \mathbf{x}_N$  and  $\mathbf{p}_{\mathbf{x}_1}, \dots, \mathbf{p}_{\mathbf{x}_N}$  is given by:

$$P(\mathbf{x}, \mathbf{p}) = \frac{1}{\mathcal{N}} \exp -\beta H$$

where  $H$  is the Hamiltonian of the system. Equation (2.1) becomes:

$$A(\xi) = -\kappa T \log \int_{S_\xi} \exp -\beta H + \kappa T \log \mathcal{N} + A_0$$

where  $S_\xi$  is the set of all  $\mathbf{x}$  and  $\mathbf{p}$  such that  $\xi(\mathbf{x}) = \xi$ .

The derivative of  $A$  can now be explicitly evaluated:

$$\frac{\partial A}{\partial \xi} = \frac{\int_{S_\xi} \frac{\partial H}{\partial \xi} \exp -\beta H}{\int_{S_\xi} \exp -\beta H} = \left\langle \frac{\partial H}{\partial \xi} \right\rangle_{S_\xi} \quad (2.2)$$

where  $\langle \rangle_{S_\xi}$  denotes the statistical average. Thus  $\frac{\partial A}{\partial \xi}$  is equal to the statistical average of the force  $-\frac{\partial H}{\partial \xi}$  acting on  $\xi$ .

To properly define the partial derivative with respect to  $\xi$ , it is necessary to introduce generalized coordinates. We define the set of functions  $q_1, \dots, q_{3N-1}$ :

$$\begin{aligned} q_1 &= q_1(\mathbf{x}_1, \dots, \mathbf{x}_N) \\ q_{3N-1} &= q_{3N-1}(\mathbf{x}_1, \dots, \mathbf{x}_N) \end{aligned}$$

such that  $(\xi, q_1, \dots, q_{3N-1})$  forms a basis equivalent to  $\mathbf{x}_1, \dots, \mathbf{x}_N$ . We mean that for each set of values  $\mathbf{x}_1, \dots, \mathbf{x}_N$  there is a unique set of values  $(\xi, q_1, \dots, q_{3N-1})$  such that:

$$\begin{aligned} \mathbf{x}_1 &= \mathbf{x}_1(\xi, q_1, \dots, q_{3N-1}) \\ \mathbf{x}_N &= \mathbf{x}_N(\xi, q_1, \dots, q_{3N-1}) \end{aligned}$$

The derivative with respect to  $\xi$  can now be defined as the derivative computed with  $q_1, \dots, q_{3N-1}$  constant:

$$\frac{\partial}{\partial \xi} = \left( \frac{\partial}{\partial \xi} \right)_{q_1, \dots, q_{3N-1}}$$

To give a more precise expression for Eq. (2.2), we need to introduce some notations.

We can define the Jacobian of this transformation, denoted  $J$ :

$$J \stackrel{def}{=} \begin{pmatrix} \frac{\partial \xi}{\partial x_1} & \frac{\partial \xi}{\partial x_2} & \dots & \frac{\partial \xi}{\partial x_N} \\ \frac{\partial q_1}{\partial x_1} & \frac{\partial q_1}{\partial x_2} & \dots & \frac{\partial q_1}{\partial x_N} \\ \dots & \dots & \dots & \dots \\ \frac{\partial q_{3N-1}}{\partial x_1} & \frac{\partial q_{3N-1}}{\partial x_2} & \dots & \frac{\partial q_{3N-1}}{\partial x_N} \end{pmatrix} \quad (2.3)$$

and its inverse  $J^{-1}$ . We denote  $Z$  the following matrix:

$$Z \stackrel{def}{=} JM^{-1}J^t$$

where  $J^t$  is the transpose of  $J$  and  $M$  is the mass matrix

$$M = \begin{pmatrix} m_1 & 0 & \dots & 0 \\ 0 & m_2 & \dots & 0 \\ \dots & \dots & \dots & \dots \\ \dots & \dots & \dots & m_N \end{pmatrix}$$

We make the assumption for simplicity that the matrix  $Z$  can be written:

$$Z = \begin{pmatrix} Z_\xi & 0 \\ 0 & Z_q \end{pmatrix} \quad (2.4)$$

$$Z_\xi \stackrel{def}{=} \sum_{k=1}^N \frac{1}{m_k} \left( \frac{\partial \xi}{\partial x_k} \right)^2 \quad (2.5)$$

where  $Z_q$  is a  $3N - 1 \times 3N - 1$  matrix.

It is well-known that if the Hamiltonian  $H$  of the system is:

$$H(\mathbf{x}, \mathbf{p}_x) = \frac{1}{2} \sum_i \frac{\mathbf{p}_{x_i}^2}{m_i} + \Phi(\mathbf{x})$$

it is possible to define an Hamiltonian for  $\xi, q_1, \dots, q_{3N-1}$ :

$$H(\xi, q, p_\xi, p_q) = \frac{1}{2} Z_\xi p_\xi^2 + \frac{1}{2} p_q^t Z_q p_q + \Phi(\xi, q) \quad (2.6)$$

We are now in position to give a more precise expression for Eq. (2.2), using Eq. (2.6):

$$\frac{\partial A}{\partial \xi} = \left\langle \frac{1}{2} \frac{\partial Z_\xi}{\partial \xi} p_\xi^2 + \frac{1}{2} p_q^t \frac{\partial Z_q}{\partial \xi} p_q + \frac{\partial \Phi(\xi, q)}{\partial \xi} \right\rangle_{S_\xi} \quad (2.7)$$

Obviously, such a formula is not very useful since we need to explicitly define the functions  $q_1, \dots, q_{3N-1}$  to compute  $\frac{\partial A}{\partial \xi}$ . The purpose of Section 2.1 is to give an equivalent form of (2.7) in which no reference is explicitly made to  $q$  and  $p_q$ .

The two following sections, Sections 2.2 and 2.3, will explain how this expression can be adapted to the case where  $\xi$  is decoupled from the other degrees of freedom and is varying in a quasi-static fashion.

### 2.1. Unconstrained simulation

In the following sections we will use the following notations:

$$\mathbf{x}'_i \stackrel{def}{=} \sqrt{m_i} \mathbf{x}_i \quad \mathbf{p}'_{\mathbf{x}_i} \stackrel{def}{=} \frac{\mathbf{p}_i}{\sqrt{m_i}} \quad (2.8)$$

$$\mathcal{H} \stackrel{def}{=} \left( \frac{\partial^2 \xi}{\partial \mathbf{x}'_i \partial \mathbf{x}'_j} \right) = \left( \frac{1}{\sqrt{m_i m_j}} \frac{\partial^2 \xi}{\partial \mathbf{x}_i \partial \mathbf{x}_j} \right) \quad (2.9)$$

Recall that

$$\frac{\partial H}{\partial \xi} = - \frac{dp_\xi}{dt} \quad (2.10)$$

$$p_\xi \stackrel{def}{=} \frac{\dot{\xi}}{Z_\xi} \quad (2.11)$$

Thus the derivative of  $H$  is equal to:

$$\frac{\partial H}{\partial \xi} = - \frac{\ddot{\xi}}{Z_\xi} + \frac{\dot{\xi}}{Z_\xi^2} \frac{dZ_\xi}{dt} \quad (2.12)$$

We now denote  $\cdot$  a dot product or a matrix-vector product. From the rules of derivation:

$$\frac{dZ_\xi}{dt} = \sum_i \frac{\partial Z_\xi}{\partial \mathbf{x}_i} \frac{d\mathbf{x}_i}{dt} = \frac{\partial Z_\xi}{\partial \mathbf{x}'} \cdot \mathbf{p}'_x \quad (2.13)$$

Using Eq. (2.12) & (2.13) and Definition (2.11):

$$\frac{\partial H}{\partial \xi} = -\frac{\ddot{\xi}}{Z_\xi} + \frac{p_\xi}{Z_\xi} \frac{\partial Z_\xi}{\partial \mathbf{x}'} \cdot \mathbf{p}'_x \quad (2.14)$$

Since

$$\mathbf{p}_x = J^t \begin{pmatrix} p_\xi \\ p_q \end{pmatrix} \quad (2.15)$$

we have:

$$\int e^{-\beta H} \frac{p_\xi}{Z_\xi} \frac{\partial Z_\xi}{\partial \mathbf{x}'} \cdot \mathbf{p}'_x dp_q = \int e^{-\beta H} \frac{p_\xi}{Z_\xi} \frac{\partial Z_\xi}{\partial \mathbf{x}'} \cdot (J')^t \begin{pmatrix} p_\xi \\ p_q \end{pmatrix} dp_q$$

As we integrate over  $p_q$  the only non-zero contribution is:

$$\int e^{-\beta H} \frac{p_\xi}{Z_\xi} \frac{\partial Z_\xi}{\partial \mathbf{x}'} \cdot (J')^t \begin{pmatrix} p_\xi \\ p_q \end{pmatrix} dp_q = \int e^{-\beta H} \frac{p_\xi^2}{Z_\xi} \frac{\partial Z_\xi}{\partial \mathbf{x}'} \cdot \frac{\partial \xi}{\partial \mathbf{x}'} dp_q$$

using Definition (2.3) of  $J$ .

Finally using Definition (2.5) of  $Z_\xi$  and Definition (2.9) of  $\mathcal{H}$ :

$$\int e^{-\beta H} \frac{p_\xi}{Z_\xi} \frac{\partial Z_\xi}{\partial \mathbf{x}'} \cdot \mathbf{p}'_x dp_q = 2 \int e^{-\beta H} \frac{p_\xi^2}{Z_\xi} \frac{\partial \xi}{\partial \mathbf{x}'} \cdot \mathcal{H} \cdot \frac{\partial \xi}{\partial \mathbf{x}'} dp_q \quad (2.16)$$

We can compute the integral over  $p_\xi$  now and obtain, using Eq. (2.6):

$$\int p_\xi^2 \exp\left(-\frac{\beta}{2} Z_\xi p_\xi^2\right) dp_\xi = \frac{1}{\beta Z_\xi} \int \exp\left(-\frac{\beta}{2} Z_\xi p_\xi^2\right) dp_\xi \quad (2.17)$$

Gathering Eqs. (2.14), (2.16), and (2.17), we have proved that

$$\frac{\partial A}{\partial \xi} = \left\langle \frac{\partial H}{\partial \xi} \right\rangle_{q, p_q, p_\xi} = \left\langle -\frac{\ddot{\xi}}{Z_\xi} + \frac{2}{\beta Z_\xi^2} \frac{\partial \xi}{\partial \mathbf{x}'} \cdot \mathcal{H} \cdot \frac{\partial \xi}{\partial \mathbf{x}'} \right\rangle_{q, p_q, p_\xi} \quad (2.18)$$

$$\ddot{\xi} = -\frac{\partial \Phi}{\partial \mathbf{x}'} \cdot \frac{\partial \xi}{\partial \mathbf{x}'} + \mathbf{p}'_x \cdot \mathcal{H} \cdot \mathbf{p}'_x \quad (2.19)$$

where  $\langle \rangle_{q, p_q, p_\xi}$  denotes an average with respect to  $q$ ,  $p_q$ , and  $p_\xi$ . We call thermodynamics force  $F_\xi$  the force defined by:

$$F_\xi \stackrel{def}{=} \frac{1}{Z_\xi} \ddot{\xi} - \frac{2}{\beta Z_\xi^2} \frac{\partial \xi}{\partial \mathbf{x}'} \cdot \mathcal{H} \cdot \frac{\partial \xi}{\partial \mathbf{x}'} \quad (2.20)$$

Equation (2.18) is very convenient from a numerical point of view since it involves only quantities which can be readily computed:  $\xi$  and its derivatives with respect to time and position.

## 2.2. Arbitrary motion along $\xi$

In SFA the motion along  $\xi$  is decoupled from the rest of the system. Then,  $\xi$  is advanced in some manner that ensures uniform sampling of  $\xi$ , for example by using Langevin equation of motion. In this new system the free energy along  $\xi$  is no longer properly defined and Equation (2.18) no longer applies. However, it is possible to compute the free energy of the original (unmodified) system, provided that the motion of  $\xi$  is quasistatic. This requires transforming Equation (2.18). Deriving the appropriate formula for  $\frac{\partial A}{\partial \xi}$  is the objective of this section.

Suppose that we run a MD simulation at fixed  $\xi = \xi_0$ . In the case of a Hamiltonian system, the probability density for  $(q, p_q, p_\xi)$  at  $\xi = \xi_0$  is equal to  $\exp(-\beta H_{\xi_0})$  where

$$H_{\xi_0}(q, p_q, p_\xi) = \frac{1}{2} Z_\xi p_\xi^2 + \frac{1}{2} p_q^t Z_q p_q + \Phi_{\xi_0}(q)$$

However, when  $\xi$  is decoupled from other degrees of freedom and advanced quasistatically using an independent equation, we sample with a probability equal to  $\exp(-\beta H_{\xi_0}^*)$ , where

$$H_{\xi_0}^*(q, p_q, p_\xi) = K^{ext}(p_\xi) + \frac{1}{2} p_q^t Z_q p_q + \Phi_{\xi_0}(q)$$

The function  $K^{ext}$  depends on the equation of motion for  $\xi$ . If this is a diffusion equation (Langevin)

$$K^{ext}(p_\xi) = \frac{1}{2} \frac{T}{T_\xi} p_\xi^2$$

where  $T_\xi$  is the temperature used in the Langevin equation (see Section 3). Because we sample from a different probability distribution function it is not possible to use Equation (2.18) directly. This difficulty can be solved by calculating analytically the integral over  $p_\xi$  in Equation (2.18). To do so we first identify the terms which depend on  $p_\xi$ : the acceleration  $\dot{\xi}$  and the probability density. More specifically considering Equation (2.18) and (2.19), we need to calculate:

$$\int f_\xi p'_x \cdot \mathcal{H} \cdot p'_x dp_\xi$$

where  $f_\xi = \exp(-\frac{\beta}{2} Z_\xi p_\xi^2)$ .

Denoting  $f_{p_q} = \exp(-\frac{\beta}{2} p_q^t Z_q p_q)$  we have:

$$\int f_{p_q} p'_x \cdot \mathcal{H} \cdot p'_x dp_q = \int f_{p_q} \begin{pmatrix} p_\xi \\ p_q \end{pmatrix} \cdot J' \mathcal{H} (J')^t \cdot \begin{pmatrix} p_\xi \\ p_q \end{pmatrix} dp_q \quad (2.21)$$

$$= p_\xi^2 \frac{\partial \xi}{\partial \mathbf{x}'} \cdot \mathcal{H} \cdot \frac{\partial \xi}{\partial \mathbf{x}'} \int f_{p_q} dp_q + \int f_{p_q} p_q \cdot J'_q \mathcal{H} (J'_q)^t \cdot p_q dp_q \quad (2.22)$$

using Equation (2.15), and the fact that integration is performed over  $p_q$ .

Next we consider the integral over  $p_\xi$  and use Equation (2.17):

$$\int f_\xi p_\xi^2 \frac{\partial \xi}{\partial \mathbf{x}'} \cdot \mathcal{H} \cdot \frac{\partial \xi}{\partial \mathbf{x}'} dp_\xi = \frac{1}{\beta Z_\xi} \frac{\partial \xi}{\partial \mathbf{x}'} \cdot \mathcal{H} \cdot \frac{\partial \xi}{\partial \mathbf{x}'} \int f_\xi dp_\xi \quad (2.23)$$

Using this equation, we observe that the following transformation is possible on statistical averages:

$$\left\langle p'_x \cdot \mathcal{H} \cdot p'_x + \left( \frac{1}{\beta Z_\xi} - \frac{\xi^2}{Z_\xi^2} \right) \frac{\partial \xi}{\partial \mathbf{x}'} \cdot \mathcal{H} \cdot \frac{\partial \xi}{\partial \mathbf{x}'} \right\rangle_{q, p_q, p_\xi} = \langle p'_x \cdot \mathcal{H} \cdot p'_x \rangle_{q, p_q, p_\xi}$$

Further, using Equation (2.22) and (2.23)

$$\begin{aligned} \left\langle p'_x \cdot \mathcal{H} \cdot p'_x + \left( \frac{1}{\beta Z_\xi} - \frac{\xi^2}{Z_\xi^2} \right) \frac{\partial \xi}{\partial \mathbf{x}'} \cdot \mathcal{H} \cdot \frac{\partial \xi}{\partial \mathbf{x}'} \right\rangle_{q, p_q, p_\xi} = \\ \left\langle \frac{1}{\beta Z_\xi} \frac{\partial \xi}{\partial \mathbf{x}'} \cdot \mathcal{H} \cdot \frac{\partial \xi}{\partial \mathbf{x}'} + p_q \cdot J'_q \mathcal{H} (J'_q)^t \cdot p_q \right\rangle_{q, p_q, p_\xi} \end{aligned}$$

We have proven the following result:

$$\int \exp(-\beta H_{\xi_0}) F_{\xi} = \int \exp(-\beta H_{\xi_0}) F_{\xi}^{(2)}$$

with  $F_{\xi}^{(2)} = \frac{1}{Z_{\xi}} \ddot{\xi} - \left( \frac{1}{\beta} + \frac{\dot{\xi}^2}{Z_{\xi}} \right) \frac{1}{Z_{\xi}^2} \frac{\partial \xi}{\partial \mathbf{x}'} \cdot \mathcal{H} \cdot \frac{\partial \xi}{\partial \mathbf{x}'}$

(see Equation (2.20) for the definition of  $F_{\xi}$ ). Moreover  $\int f_{p_q} F_{\xi}^{(2)} dp_q$  is independent of  $p_{\xi}$ . Thus, we have removed the dependence of the average force on  $p_{\xi}$ . This is a desirable result because the dependence on  $p_{\xi}$  changes with implementation of quasistatic process. Thus we can conclude:

$$\int dp_{\xi} f_{\xi} \int dp_q f_{p_q} F_{\xi}^{(2)} = \int dp_q f_{p_q} F_{\xi}^{(2)} \times \int dp_{\xi} \exp\left(-\frac{\beta}{2} Z_{\xi} p_{\xi}^2\right) \propto \frac{1}{\sqrt{Z_{\xi}}} \int dp_q f_{p_q} F_{\xi}^{(2)}$$

We proved that when  $\xi$  is decoupled and moves quasistatically, the following equation applies:

$$\frac{\partial A}{\partial \xi} = \frac{\left\langle \frac{1}{\sqrt{Z_{\xi}}} F_{\xi}^{(2)} \right\rangle_{q,p_q}}{\left\langle \frac{1}{\sqrt{Z_{\xi}}} \right\rangle_{q,p_q}} = \frac{\left\langle \frac{-1}{Z_{\xi}^{3/2}} \ddot{\xi} + \left( \frac{1}{\beta} + \frac{\dot{\xi}^2}{Z_{\xi}} \right) \frac{1}{Z_{\xi}^{5/2}} \frac{\partial \xi}{\partial \mathbf{x}'} \cdot \mathcal{H} \cdot \frac{\partial \xi}{\partial \mathbf{x}'} \right\rangle_{q,p_q}}{\left\langle \frac{1}{\sqrt{Z_{\xi}}} \right\rangle_{q,p_q}} \quad (2.24)$$

where  $A$  is the free energy of the original system.

### 2.3. Constrained simulation

The case of the constrained simulation is a corollary of the previous result. It is a particular case of a ‘‘quasi-static’’ motion where the velocity of  $\xi$  is zero.

In this case  $F_{\xi}^{(2)}$  is simply equal to:

$$F_{\xi}^{(2)} = \frac{-1}{Z_{\xi}} \ddot{\xi} + \frac{1}{\beta} \frac{1}{Z_{\xi}^2} \frac{\partial \xi}{\partial \mathbf{x}'} \cdot \mathcal{H} \cdot \frac{\partial \xi}{\partial \mathbf{x}'}$$

Thus the complete expression for  $\frac{\partial A}{\partial \xi}$  is

$$\frac{\partial A}{\partial \xi} = \frac{\left\langle \frac{-1}{Z_{\xi}^{3/2}} \ddot{\xi} + \frac{1}{\beta} \frac{1}{Z_{\xi}^{5/2}} \frac{\partial \xi}{\partial \mathbf{x}'} \cdot \mathcal{H} \cdot \frac{\partial \xi}{\partial \mathbf{x}'} \right\rangle_{q,p_q}}{\left\langle \frac{1}{\sqrt{Z_{\xi}}} \right\rangle_{q,p_q}} \quad (2.25)$$

This expression is identical to Otter and Briels (1998).

## 3. Description of the algorithm

At each timestep we need to calculate the force along  $\xi$ , which is of the form  $\lambda(t) \frac{\partial \xi}{\partial \mathbf{x}}$ . This is the centerpiece of SFA. The force must be such that:

$$Z_{\xi} \lambda(t) - \frac{\partial \Phi}{\partial \mathbf{x}'} \cdot \frac{\partial \xi}{\partial \mathbf{x}'} + p'_{\mathbf{x}} \cdot \mathcal{H} \cdot p'_{\mathbf{x}} = 0$$

To compute the value of  $\lambda(t)$  we use a modified version of RATTLE, for which the ‘‘constraints’’ are updated at each timestep.



Consider the traditional RATTLE algorithm and suppose that we have a constraint  $\sigma(\mathbf{x}) = \sigma_0$ , which has to be satisfied at each timestep. The algorithm consists of two steps. After advancing the position from time  $t$  to  $t + dt$ , RATTLE is used to compute the force  $\mu^r \nabla \sigma$ , such that  $\sigma(\mathbf{x}(t + dt)) = \sigma_0$ . After advancing the velocity from time  $t + dt/2$  to  $t + dt$ , RATTLE is used to compute the force  $\mu^v \nabla \sigma$ , such that  $v \cdot \nabla \sigma = 0$ .

In contrast, in SFA we need to add a force which exactly compensates the acceleration of  $\xi$  due to the interatomic forces. Since the constraint has to be changed at each timestep the algorithm is slightly different. After advancing the position from time  $t$  to  $t + dt$ , RATTLE is used to compute the force  $\lambda^r \nabla \xi$ , such that  $\xi(t + dt) = \xi(t) + dt \dot{\xi}(t)$ , where  $\dot{\xi}(t)$  is the velocity before the forces are applied at time  $t$ . After advancing the velocity from time  $t + dt/2$  to  $t + dt$ , RATTLE is used to compute the force  $\lambda^v \nabla \xi$ , such that  $v \cdot \nabla \xi(t + dt) = \dot{\xi}(t + dt) = \dot{\xi}(t)$ , where  $\dot{\xi}(t)$  is the velocity before the forces are applied at time  $t$ .

Once  $\xi$  is decoupled from the other degrees of freedom, we apply a Langevin force to  $\xi$  so that we obtain a diffusive motion along  $\xi$ . We define  $\mu(t)$  with:

$$\mu(t) = -\zeta \dot{\xi} + R(t)$$

and

$$\langle R(t)R(t') \rangle = 2\zeta kT_\xi \delta(t - t')$$

where  $\zeta$  is friction coefficient,  $R(t)$  is normally distributed random force, whose ensemble average is zero, and  $T_\xi$  is the temperature. Note that  $\zeta$  is related to the diffusion constant,  $D$ , by the Einstein relation:

$$D = kT/\zeta$$

The total external force applied to the system is equal to the RATTLE force plus the Langevin force:

$$\left( \lambda(t) + \frac{\mu(t)}{Z_\xi} \right) \frac{\partial \xi}{\partial \mathbf{x}}$$

### 3.1. RATTLE Lagrange multipliers

In this section the equations for  $\lambda^r$  and  $\lambda^v$  the position and velocity Lagrange multiplier for RATTLE are given. We will show that  $\lambda^r$  can be used to compute the value of  $\dot{\xi}$ .

Let us consider the position RATTLE. The position is advanced using:

$$r(t + dt) = r(t) + v(t + dt/2)dt \quad (3.1)$$

while the velocity is advanced using:

$$v(t + dt/2) = v(t) + \frac{dt}{2} \frac{F(t)}{m} \quad (3.2)$$

After position RATTLE is applied we want  $\xi$  to be equal to:

$$\xi^R(t + dt) = \xi(t) + dt \dot{\xi}(t) \quad (3.3)$$

Using a Taylor-Lagrange approximation, we obtain the equation for  $\lambda^r$ :

$$\lambda^r(t) = \frac{-dt}{2Z_\xi(t)} \left( \frac{F(t)}{m} \nabla \xi + v(t) \cdot \mathcal{H} \cdot v(t) \right) = \frac{dt}{2} \frac{-\ddot{\xi}(t)}{Z_\xi} \quad (3.4)$$

See Eq. (2.19). This equation means that  $\lambda^r$  can be used to compute the value of  $\ddot{\xi}$  at each time-step.

For velocity RATTLE we have a similar equation. For the velocity:

$$v(t+dt) = v(t) + \frac{dt}{2} \frac{F(t)}{m} + \lambda^r \frac{\nabla \xi(t)}{m} + \frac{dt}{2} \frac{F(t+dt)}{m} \quad (3.5)$$

$$v^R(t+dt) = v(t+dt) + \lambda^v \frac{\nabla \xi(t+dt)}{m} \quad (3.6)$$

As the constraint on  $v^R(t+dt)$  is  $v^R(t+dt) = v(t)$  we obtain:

$$\lambda^v = \frac{-dt}{2Z_\xi(t+dt)} \left( \frac{F(t)}{m} \nabla \xi + \frac{2}{dt} \lambda^r \frac{\nabla \xi(t) \cdot \nabla \xi(t+dt)}{m} + \frac{F(t+dt)}{m} \nabla \xi \right)$$

At first order using Eq. (3.4):

$$\begin{aligned} \lambda^v(t) &= \frac{-dt}{2Z_\xi(t+dt)} \left( \frac{F(t)}{m} \nabla \xi + \frac{2Z_\xi(t)}{dt} \lambda^r + \frac{F(t+dt)}{m} \nabla \xi \right) \\ &= \frac{-dt}{2Z_\xi(t+dt)} \left( \frac{F(t+dt)}{m} \nabla \xi - v(t) \cdot \mathcal{H} \cdot v(t) \right) \end{aligned}$$

Note that only  $\lambda^r$  is equal to  $-\frac{dt}{2} \frac{\ddot{\xi}(t)}{Z_\xi}$ . For  $\lambda^v$  the sign in front of  $v(t) \cdot \mathcal{H} \cdot v(t)$  is opposite.

#### 4. Application - isomerization of 1,2-dichloroethane in water

To test the performance of the SFA, we studied the rotation around the C-C bond in 1,2-dichloroethane (DCE) dissolved in water. Specifically, we calculated the free energy  $A(\xi)$  as a function of the Cl-C-C-Cl torsional angle  $\xi$ . The same quantity was previously calculated for DCE in several different environments, including the gas phase, bulk water, bulk Hexane, and water-Hexane interface, using conventional methods (Benjamin and Pohorille (1993), Pohorille and Wilson (1993)). See Fig. 2. In all environments,  $A(\xi)$  exhibits local minima corresponding to the trans and gauche arrangements of the chlorine atoms. However, the relative stabilities of these two conformations and the free energy barrier that separates them change with environment. The trans conformation was found to be favored by 1.1 kcal/mol in the gas phase, whereas gauche conformations were slightly favored in water (by 0.3 kcal/mol) (Benjamin and Pohorille (1993), Pohorille and Wilson (1993)). The shift of 1.4 kcal/mol stabilizing the gauche conformations in aqueous solutions can be attributed to strong, favorable interactions between these polar conformations and water. Note that the symmetrical, trans conformation has no permanent dipole moment. Also, the free energy barrier between the gauche and trans states increased from 3.5 kcal/mol in the gas phase to 4.4 kcal/mol in aqueous solution. This indicates that the solvent provides a considerable contribution to the potential of mean force around  $\xi$ .

The system studied consisted of one DCE molecule and 343 water molecules placed in a cubic box whose edge length was 21.73 Å. This corresponds to a water density of approximately 1 g/cm<sup>3</sup>. Periodic boundary conditions were applied in the three spatial directions. The water-water interactions were described by the TIP4P potential model (Jorgensen (1983)). For DCE, an all-atom, fully flexible model was used. This model was described in detail previously (Benjamin and Pohorille (1993)). All intermolecular

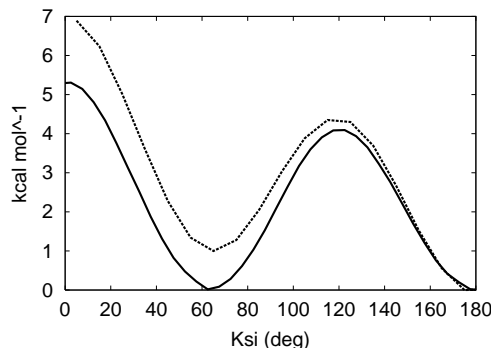


FIGURE 2. DCE in different environments: gas phase (.....) and in bulk water (—). These free energies were computed with a traditional window method.

interactions were truncated smoothly with a cubic spline function between 8.0 and 8.5 Å.

The MD equations of motion were integrated using the velocity Verlet algorithm with a time step of 1 fs. The temperature of the system was 300 K. The bond and angular constraints were resolved using RATTLE (Andersen (1983)). The same algorithm was also used to calculate the force of constraint acting on  $\xi$  whenever necessary. To generate configurations from the canonical ensemble, the Martyna *et al.* implementation (Martyna (1992)) of the Nose-Hoover algorithm was used.

Initially, we performed simulations of the system without scaling ( $\alpha=1$ ) in both microcanonical and canonical ensembles.  $A(\xi)$  was obtained from a series of calculations in which  $\xi$  was constrained by a harmonic potential in 2 overlapping windows. The MD trajectory for each window was 1.0 ns long. From this trajectory the probability distribution,  $P(\xi)$ , of finding DCE in a conformation defined by  $\xi$  was obtained and used to calculate  $A(\xi)$  from Equation (2.1).

The free energy profile in the full range of  $\xi$  was generated by matching  $A(\xi)$  in the overlapping regions of consecutive windows. This was required to ensure that  $A(\xi)$  was a continuous function of  $\xi$ . Matching was done using the Weighted Histograms Method (Kumar (1992)).

The free energy profiles in the microcanonical and canonical ensembles were nearly identical and were quite similar to those calculated previously using the same potential functions (Benjamin and Pohorille (1993), Pohorille and Wilson (1993)). Gauche and trans conformations were found to have nearly the same free energy and were separated by a barrier 4.2 kcal/mol high. The profiles, shown in Fig. 3, served as the reference to determine accuracy of the SFA. Their statistical precision was further confirmed by fitting a Fourier series to  $A(\xi)$  and repeating the calculations using the series as the biasing potential. As expected, the free energy profile so generated was flat. The same calculations were also used to estimate the rotational diffusion constant,  $D$ , needed for the Langevin term in SFA. This was done by calculating the velocity autocorrelation function and employing the formula:

$$D = \frac{1}{2} \int_0^{\infty} \langle v(0)v(t) \rangle,$$

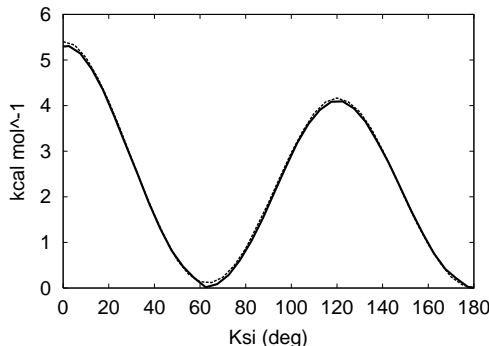


FIGURE 3. DCE in bulk water. This figure shows the reference result, computed with a traditional window method (—), and SFA with a biasing potential (⋯).

where  $v(t)$  is the velocity of the torsional angle and  $\langle \dots \rangle$  denotes a statistical average. The diffusion coefficient was computed to be  $0.53 \text{ rad}^2/\text{ps}$ .

In the next step, we compute the free energy using Eq. (2.18) and not the probability density (Eq. (2.1)). In this simulation (Fig. 3), we use the original interaction forces and add a biasing potential to the system to obtain a uniform sampling. At every MD step, the values of the constraint force (i.e. obtained using RATTLE) are binned in small intervals of  $\xi$ , and at the end of the simulation, the average value of the force of constraint in each bin is calculated. Next, these values are corrected for the geometrical factor according to Eq. (2.18), yielding the thermodynamic force as a function of  $\xi$ . This force is then integrated numerically to provide  $A(\xi)$ .

The important point is that we are still in a Hamiltonian framework which guarantees a convergence to the exact solution as the simulation time goes to  $+\infty$ .

The simulation was run for 1 ns and the resulting free energy profile is shown in Fig. 3 and compared with the profile obtained from the previous calculations and Eq. (2.1). As can be seen, the agreement between the two profiles is excellent.

Then, simulations of the same system are performed using SFA with  $\alpha = 1$ . This means that the angle  $\xi$  is fully decoupled from the rest of the system. To advance this angle the Langevin equation of motion is integrated. We choose different diffusion coefficients. In this table we summarize the run times and number of windows used:

Diffusion Coefficient	Number of windows	Simulation time
$0.53 \text{ rad}^2/\text{ps}$	1	1ns
$0.53 \times 10^{-1} \text{ rad}^2/\text{ps}$	1	1ns
$0.53 \times 10^{-2} \text{ rad}^2/\text{ps}$	2	1ns
$0.13 \times 10^{-2} \text{ rad}^2/\text{ps}$	3	2ns

The simulation time is per window. The number of windows and simulation time have to be increased because as the diffusion constant goes to zero it takes more and more time to cover the complete range from 50 deg to 190 deg.

For this simulation we use Eq. (2.24) to compute the free energy. This is the equation

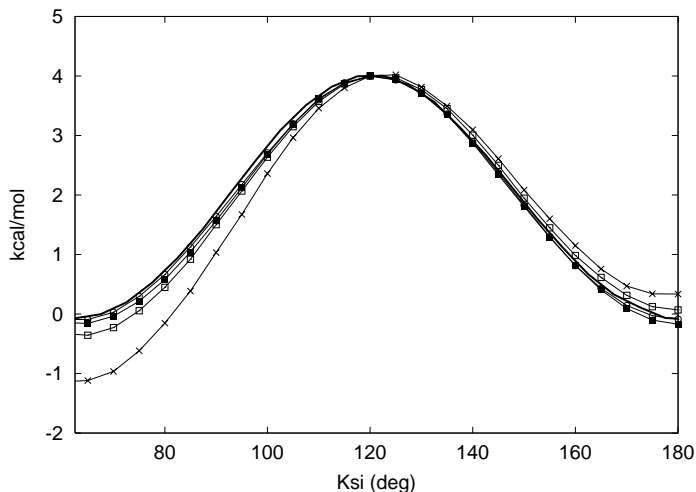


FIGURE 4. DCE in bulk water. These are the results obtained with SFA using a Langevin force with different diffusion constants:  $0.53$  ( $\text{---}\times\text{---}$ ),  $0.53 \times 10^{-1}$  ( $\text{---}\square\text{---}$ ),  $0.53 \times 10^{-2}$  ( $\text{---}\blacksquare\text{---}$ ) and  $0.13 \times 10^{-2}$   $\text{rad}^2/\text{ps}$  ( $\text{---}\circ\text{---}$ ). The reference curve ( $\text{---}\blacksquare\text{---}$ ) is shown with a thick line. Only the range  $[60-180]$  degrees was computed. Note that since the free energy is defined up to a constant, we decided to align all the curves at the point  $\xi = 120$  deg. The fact that the difference with the reference curve is more significant at  $60$  deg than  $180$  deg reflects the fact that the precise shape of the free energy around  $60$  deg depends on precise interactions with the water and correct equilibration at these configurations.

that we need to use when  $\xi$  is decoupled from the other degrees of freedom and advanced in a quasi-static manner.

For these simulations we no longer have a Hamiltonian system. The free energy profile converges to the exact solution only when  $\xi$  is a sufficiently “slow” degree of freedom. This means that  $\xi$  has to change in a quasi-static way to get a correct convergence. If it changes sufficiently fast that the rest of the rest of the system cannot relax in response to its movements, the system is in a non-equilibrium state and the free energy converges to the wrong value.

We progressively lower the diffusion coefficient and observe that the free energy converges to the exact solution as the motion of  $\xi$  becomes quasi-static. The results are shown in Fig. 4.

## 5. Conclusion and future work

We developed a new method called Scaled Force Algorithm to compute free energies. It is based on decoupling the reaction coordinates from the other degrees of freedom. The free energy of the original system can then be computed using Eq. (2.24). The advantage of the method is that the sampling is guaranteed to be homogeneous, which is the best possible sampling to minimize CPU time.

We made two kinds of computations. In the first we applied a biasing potential and the system was Hamiltonian. In this case, the general theory of Hamiltonian system applies and the computed free energy (with Eq. (2.18)) converges to the exact free energy when the simulation time goes to  $+\infty$ . In the second we applied a Langevin force and the system was not Hamiltonian. In this case we need to satisfy a quasi-static hypothesis to converge towards the exact free energy (Eq. (2.24)).

We are currently developing a new method, the Adaptive Biasing Force, which has two main advantages:

- The system converges towards a Hamiltonian system. We are thus guaranteed to converge towards the exact free energy regardless of the quasi-static hypothesis. This is an advantage over the Langevin force variant.
- The Adaptive Biasing Force is computed as the simulation goes and thus no a priori guess is needed. This is an advantage over the biasing potential variant.

Early tests confirm that the new method will yield even better results than the ones presented in this report (biasing potential and Langevin force).

We are also planning to study two-dimensional or multi-dimensional cases where the number of slow degrees of freedom is two or more.

A very important application of the method is the problem of protein folding. The solution of these problems has so far been limited because the computational time is extremely large. A full computation requires on the order of  $10^9$  time-steps to reach the micro-second time-scale. Such a large number of time-steps results from the fact that the system has to cross energy barriers between intermediate steps of the folding. SFA will allow to lower these energy barriers and thus reduce the computational time of the solution.

#### REFERENCES

- ANDERSEN., H. C. 1983 Rattle: a ‘velocity’ version of the shake algorithm for molecular dynamics calculations. *J. Comput. Phys.* **52**, 24-34.
- BENJAMIN, I. & POHORILLE, A. 1993 Isomerization reaction dynamics and equilibrium at the liquid-vapor interface of water — a molecular dynamics study. *J. Chem. Phys.* **98**, 236-242.
- DEN OTTER, W. K. & BRIELS, W. J. 1998 The calculation of free-energy differences by constrained molecular-dynamics simulation. *J. Chem. Phys.* **109(11)**, 4139-4146.
- JORGENSEN, W. L., CHANDRASEKHAR, J., MADURA, J. D., IMPEY, R. W. & KLEIN, M. L. 1983 Comparison of simple potential functions for simulating liquid water. *J. Chem. Phys.* **79**, 926-935.
- KUMAR, S., BOUZIDA, D., SWENDSEN, R. H., KOLLMAN, P. A. & ROSENBERG, J. M. 1992 The weighted histogram analysis method for free-energy calculations on biomolecules 1: The method. *J. Comput. Chem.* **13**, 1011-1021.
- MARTYNA, G. J., KLEIN, M. L. & TUCKERMAN, M. 1992 Nose-Hoover chains — the canonical ensemble via continuous dynamics. *J. Chem. Phys.* **97**, 2635-2643.
- POHORILLE, A. & WILSON, M. A. 1993 Isomerization reactions at aqueous interfaces. In Jortner, J., Levine, R. D. & Pullman, B. editors, *Reaction Dynamics in Clusters and Condensed Phases — The Jerusalem Symposia on Quantum Chemistry and Biochemistry*, **26**, 207, Kluwer, Dordrecht.